Effects of particle size on the separation efficiency in a rotary-drum eddy current separator

Cao Bin[a,b,c], Yuan Yi[a*], Shan Zhicheng[a,b], Wang Qiang[b], Amor Abdelkader[c], Ali Reza Kamali[a,d], Diogo Montalvão[c]

(a School of Metallurgy, Northeastern University, Shenyang 110819, China

b Key Laboratory of Electromagnetic Processing of Materials (Ministry of Education), Northeastern University, Shenyang 110819, China

c Department of Design and Engineering, Faculty of Science & Technology, Bournemouth University, Poole, Dorset BH12 5BB, United Kingdom

d Energy and Environmental Materials Research Center (E^2MC), Northeastern University, Shenyang 110819, China.)

*Corresponding author: Yuan Yi. Tel. 86-024-83681171; Fax: 86-024-83681758. E-mail address: yuany@smm.neu.edu.cn.

Abstract: Eddy current separation is a technology for recovering non-ferrous metals. The influence of particle size on the separation is of significant importance due to the variety of materials. It was investigated by combining simulations and physical experiments. A strong correlation between the simulation and the experiment was found by Pearson correlation analysis. Then the interaction effects between the particle size and the material type, rotational speed, magnetic pole arrangement were investigated. It shows that an optimal particle size exists for a specific condition, and the separation efficiency of fine particles can be improved by increasing rotational speed, magnetic pole number, and the electrical conductivity/density of material, as well as utilizing torque of Lorentz force. The underlying mechanism of particle size affecting separation was discovered by analyzing eddy current distribution and field gradient. These results provide insight into the design and optimization of eddy current separation for particles of various sizes.

Keywords: Particle size; eddy current separation; numerical simulation; Lorentz force; magnetic dipole

1. Introduction

Solid waste recycling has become one of the most important processes to the environmental protection and the sustainable use of resources and energy [1]. Furthermore, the recovery of metallic components in solid wastes is of great economic value, which has attracted increasing attention worldwide. In the metal recovery process, mechanical and physical separation methods such as optical separation, gravity separation, and electromagnetic separation are usually used to complete the upgrading process of various materials before the refining operation [2]. Optical separation methods can be used for the separation of various material types [3], but they are usually only suitable for mixtures with large particle size (>10 mm), and the equipment is also relatively expensive. Gravity separation methods are suitable for materials with sufficiently differences in density or particle size [4]. Electromagnetic separation methods, mainly including electrostatic separation [5], magnetic separation [6] and eddy current separation, are capable of processing mixtures with a wide range of particle sizes, appropriate for a wide variety of solid wastes. The last two are usually used together on the same production line: the ferromagnetic metals are separated from the mixture by magnetic separator, and then non-ferrous metals and non-metallic materials are separated by eddy current separator (ECS) [7].

In ECS, Lorentz force (F_{eddy}) is responsible for separating non-ferrous metal particles from other materials [8]. There are two recognitions for the Lorentz force in eddy current separation: (1) the eddy current in the conductive particle is induced under the alternating magnetic field, and the eddy current further interacts with the alternating magnetic field to generate a repulsive force; (2) the alternating magnetic field induces eddy current in the conductive particle, and the derived magnetic field generated by the eddy current interacts with the alternating magnetic field to form a repulsive force. The theoretical models were developed based on the above two recognitions respectively [9]. This technology has the advantages of low energy consumption, large processing capacity, easy operation, and no secondary pollution. It is the most suitable separation technology for large-scale recycling of non-ferrous metals [9], and has been widely used to process various mixtures including the electronic waste [10], incinerator bottom ash [11], automotive shredder residue, foundry sand, etc [12]. Moreover, some researchers are also trying to use the principle of ECS to manipulate and clean up the space debris [13]. Despite the advantages mentioned above, the ECS suffers poor separation efficiency for mixtures consisting of fine particles (<5 mm), significantly restricting the further development of eddy current separation technology [8]. Improving the separation efficiency of mixtures with various particle sizes in ECS can create a considerable deal of social and economic benefits. For example, more than 10 million tons of bottom ash, containing 5-8% metals, are generated annually in China through the incineration of municipal solid waste. Around 78% of the Cu present in the bottom ash with a particle size of less than 5 mm, which is directly discarded due to the poor separation efficiency of the ECS [14]. As another example, electronic wastes need to be crushed to achieve the liberation of various materials like metals and plastics before the separation. The statistical results show that when the printed circuit boards are crushed below 6 mm, ferromagnetic particles and Cu can be completely liberated [15]. Therefore, the effective separation of the fine particles is key to recycling electronic wastes.

To solve the challenges associated with the low separation efficiency of ECS for fine particles, some researchers have suggested increasing the Lorentz force by adjusting the intensity and frequency of the alternating magnetic field. High-frequency electromagnetic ECS (50~100 kHz) was used to separate fine particles [16]. The recovery rate of Al, Cu, and Zn particles (0.8~4 mm) could exceed the value of 85% under appropriate parameters. Despite the desirable outcomes, the utilization of such equipment at large scales is challenging, due to the fact that the mixture is separated in a narrow air gap, with a processing capacity of 50 kg/h [17]. A superconducting ECS [18] with a center field intensity of up to 5 T has also been suggested to increase the efficiency of the process, but the separation effect is yet to be confirmed by experiments. Another approach is based on the rotational motion generated by the torque of Lorentz force (T_{eddy}) to achieve the separation of fine particles. This is known that the rotational angular velocity of small non-ferrous metal particles in an alternating magnetic field can reach about 1000 rad/s [19]. Therefore, when the rotating particle pass through fluids such as air, the particle trajectory is affected by the Magnus force [20], resulting in additional deflection. The separation of non-ferrous metal particles in air and water was studied by employing this mechanism [21]. It was found that the Magnus effect can increase the recovery rate and grade of Cu particles by about 4%. In addition, a bottom-feeding ECS was proposed [22]. In this type of ECS, the non-ferrous metal particles are affected by the torque of Lorentz force, causing the non-ferrous metal particles to roll forward and jump, which is helpful to improve the separation of fine particles. However, the utilization of torque of Lorentz force is susceptible to the influence of particle shape, thus the grade and recovery rate of separation are low, limiting the industrial applications of these techniques. Other researchers tried to reduce the critical conditions required to achieve the separation through the implementation of smart structures and process arrangements. For example, the single-disk ECS requires only a short jump of non-ferrous metal particles under the action of Lorentz force to achieve effective separation [23]. Moreover, when feeding mixtures with high humidity in a traditional belted-drum ECS. The Lorentz force only needs to be greater than the adhesion force between the particles and the belt, or the liquid bridge can be broken by the rotation motion of the particles, to achieve effective separation [19]. However, the processing capacity of these ECS is small, and the industrial application of such complicated devices can be challenging.

At present, the structure that the market still favors is the traditional belted-drum

ECS [8]. In the belted-drum ECS, the research on particle size mostly adopts the research method of separation experiment. These studies have clarified the influence of particle size on repulsion distance (D_r) [24], grade, and recovery rate [25], but the underlying mechanisms governing the separation are still unclear, which is an important reason for the low separation efficiency of fine particles. To better understand the mechanisms by which the particle size affecting the separation, the electromagnetic and dynamic responses of non-ferrous metal particles should be investigated. In ECS, the trajectories of non-ferrous metal particles are simultaneously affected by Lorentz force and torque, gravity, aerodynamic drag force, Magnus effect, etc. And the dynamic variation of eddy current in non-ferrous metal particles is complicated. It is difficult to observe or measure the electrodynamic behavior of non-ferrous metal particles in separation experiments, so some researchers used numerical simulations. Bin et al. [26] studied the relationship between the magnetic roller structure and the distribution characteristics of the magnetic field based on finite element analysis (FEA). Huang et al. [27] proposed that there is no size limitation for the non-ferrous metals in eddy current separation by simulating and analyzing the magnetic field of magnetic poles based on FEA. Zhang et al. [28] studied the influence of particle size on the repulsion distance through an iterative simulation model based on the magnetic dipole theory. Ayad et al. [29] used a 2D simulation model based on FEA to study the effects of conductivity and particle size on the Lorentz force and eddy current. However, these simulation models use simplified 2D geometric model, or ignore the effect of torque of Lorentz force, and do not establish a relationship between the separation efficiency indicator and the physical quantities in the simulation. A three-dimensional transient simulation model of ECS has been established and verified in our previous research on material temperature [30]. It can provide more detailed information such as Lorentz force and torque, eddy current, etc.

In this study, the relationship between several key physical quantities in the numerical simulation and separation experiment was analyzed. On this basis, the influence of particle size on the separation efficiency and the related mechanisms were further studied. The research results can provide guidance for the design and optimization of eddy current separators.

2. Materials and methods

To systematically evaluate the impact of particle size on separation efficiency in eddy current separation, the combination of numerical simulation and experiment was used in this study. This section describes in detail the numerical simulation model and the separation experimental process.

2.1 Three-dimensional transient simulation model of ECS

In this study, a self-designed rotary-drum ECS (Fig. 1 (a)) was used as a prototype, and the corresponding three-dimensional transient simulation model of ECS was built based on FEA, as shown in Fig. 1 (b). The rotary-drum ECS is mainly composed of a magnetic roller, an electric motor, a control cabinet, and a frame. It is simplified as a rotating magnetic roller structure including an iron core and permanent magnets in the simulation model to ensure that the computational workload and accuracy of the numerical simulation are within a reasonable range. The magnetization direction of the red permanent magnet (N pole) on the magnetic roller is radially outward, while the magnetization direction of the light green permanent magnet (S pole) is radially inward. N52 grade permanent magnets were used. There are two magnetic pole arrangements of NNSS and NS set on the magnetic roller in the simulation model, which is consistent with that in the rotary-drum ECS.

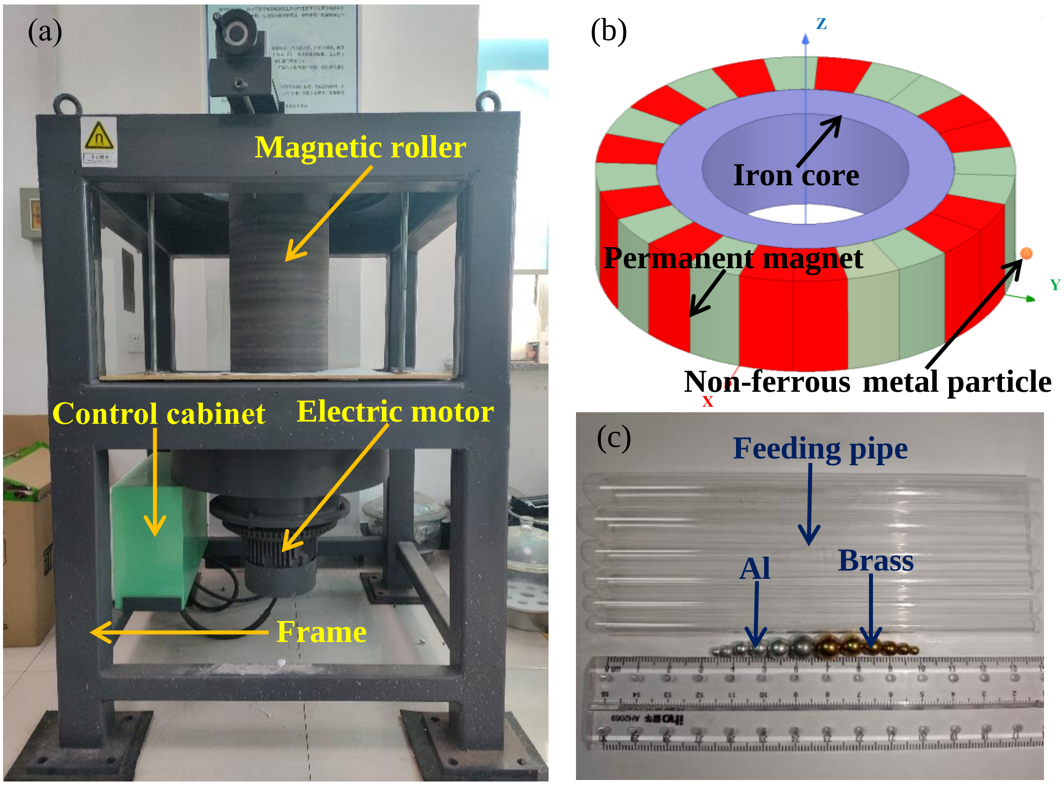

Fig. 1. (a) The rotary-drum ECS; (b) the three-dimensional transient simulation model of ECS; (c) the feeding pipe and non-ferrous metal particles for physical experiment.

Solving an electromagnetic field problem is always based on solving Maxwell's equations. However, the process of obtaining the solution is typically based on solving a second order consequence of Maxwell's equations with the consideration of applicable constitutive equations. The following constitutive relationship is relevant for the magnetic field of the magnetic poles:

$$\vec{B} = \mu_0(\vec{H} + \vec{M}) \tag{1}$$

where $\vec{B}(x, y, z)$ is the magnetic flux density. $\vec{H}(x, y, z)$ is the magnetic field strength. $\vec{M}(x, y, z)$ is the permanent magnetization. $\mu_0 = 4 \cdot \pi \cdot 10^{-7} H/m$ is the permeability of vacuum. The component of the Lorentz force due to current in a magnetic field is given by the following equation:

$$\mathrm{F}_{eddy} = \int_V J \times B dV \tag{2}$$

where J is the current density, and V is the volume of the particle. The system uses Lorentz forces to compute the torque around each axis, and the torque of Lorentz force on the particle is:

$$\mathrm{T}_{eddy} = \int_V \gamma \times (J \times B) dV \tag{3}$$

where γ is the displacement vector from the rotation axis.

In the simulation model, the rotational speed of the magnetic roller can be adjusted according to the design. The frequency of the magnetic field around the magnetic roller increases with the increase of rotational speed. Non-ferrous metal particles with different sizes are set to be next to the rotating magnetic roller, so that the electrodynamic state of the non-ferrous metal particles in an alternating magnetic field can be simulated. The master-slave boundary condition is adopted on the two ends of the magnetic roller in the axial direction, which can eliminate the error caused by the end effect of the magnetic roller, thus greatly reduce the axial length of the magnetic roller in the simulation model. In addition, some parameters such as the time step and circumferential boundary used in the simulation model were determined by the independence verification. The simulation model can be used to obtain the physical quantities such as eddy current, Lorentz force and torque of the non-ferrous metal particles near the rotating magnetic roller under different conditions. It should be noted that the simulation model in this study does not include the effects of gravity and aerodynamic drag forces. The premise of studying these forces is to achieve the coupling of finite element analysis and computational fluid dynamics, which will be the focus of our future work. The specific geometric structure and simulation parameters are shown in Table 1.

Table 1. Parameters used in the simulations.

Category		Values
Permanent magnet	Inner radius (mm)	98
	Outer radius (mm)	138
	Height (mm)	70
	Magnetic pole pairs	9
	Remanence (T)	1.43
Back iron	Inner radius (mm)	68
	Outer radius (mm)	98
	Height (mm)	70
	Relative permeability	4000
Non-ferrous metal particle	Particle size (mm)	1-32
Rotational speed of roller (rpm)		1200-6000
Time step (ms)		0.01-0.05

2.2 Separation experiment method

The separation experiment was also carried out to clarify the relationship between the Lorentz force in the simulation and the repulsion distance in the separation experiment. The rotary-drum ECS was used to carry out the separation experiments under different particle sizes, material types and rotational speeds. The specific experimental parameters are shown in Table 2.

Table 2. Parameters used in the experiments.

Material type	Rotational speed (rpm)	Particle size (mm)
Al	1800	3, 4, 5, 6, 7, 8
	3000	3, 4, 5, 6, 7, 8
Brass	3000	3, 4, 5, 6, 7, 8

In eddy current separation, particle motion includes translational motion and rotational motion. Since the Lorentz force is proportional to the magnetic flux area, the trajectories of particles with asymmetric shapes are affected by their own shapes and have stronger randomness, so spherical particles were used in the separation experiments. Al and brass, which are the most common non-ferrous ingredients of industrial solid wastes, were used. To minimize the influence of the initial state of particles on the results of the separation experiment, feeding pipes with the same length and different tube diameters were set in the feeding area, and the non-ferrous metal particles of various sizes pass through the feeding pipe before entering the separation area. The particles with diameters of 3-8 mm were matched with the feeding pipes with tube diameters of 4-9 mm and wall thickness of 1 mm, as shown in Fig. 1 (c). Feeding pipes were used to reduce random errors caused by the manual operation during feeding, so that particles of different sizes and materials can maintain a relatively consistent initial movement state and spatial position before entering the separation area. The non-ferrous metal particles are deflected by the Lorentz force and torque in the separation area. There are some pre-set scale marks in the landing area, and the whole process was filmed at 60 Hz by a video camera, and then the repulsion distance can be measured by analyzing the film frame by frame. The separation experiments under the same experimental condition were repeated at least 15 times, which can further reduce the experimental error. The experimental data of these repulsion distances meet the characteristics of normal distribution. And the average value represents the distance that the non-ferrous metal particles are thrown out by the Lorentz force, so it can directly reflect the separation efficiency between non-ferrous metal particles and non-metallic particles [24]. The standard deviation of the repulsion distance represents the concentration of the particle falling points, which is very critical when evaluating the separation effect between different non-ferrous metals.

3. Results and discussion

3.1 Correlation between simulations and separation experiments

In the simulations, many physical quantities that are difficult to measure in the separation experiments can be relatively easily obtained. However, when applying the simulation model, the connection between several key physical quantities in the simulation and separation experiment should be established to ensure that some quantities in the simulation model have physical meaning. Lorentz force is the power source that drives the non-ferrous metal particles to move in translation and deviate from other materials, so it is a very critical physical quantity in the eddy current separation. In the separation experiment, the Lorentz force is difficult to measure, but the specific value of the Lorentz force can be obtained conveniently in the simulation.

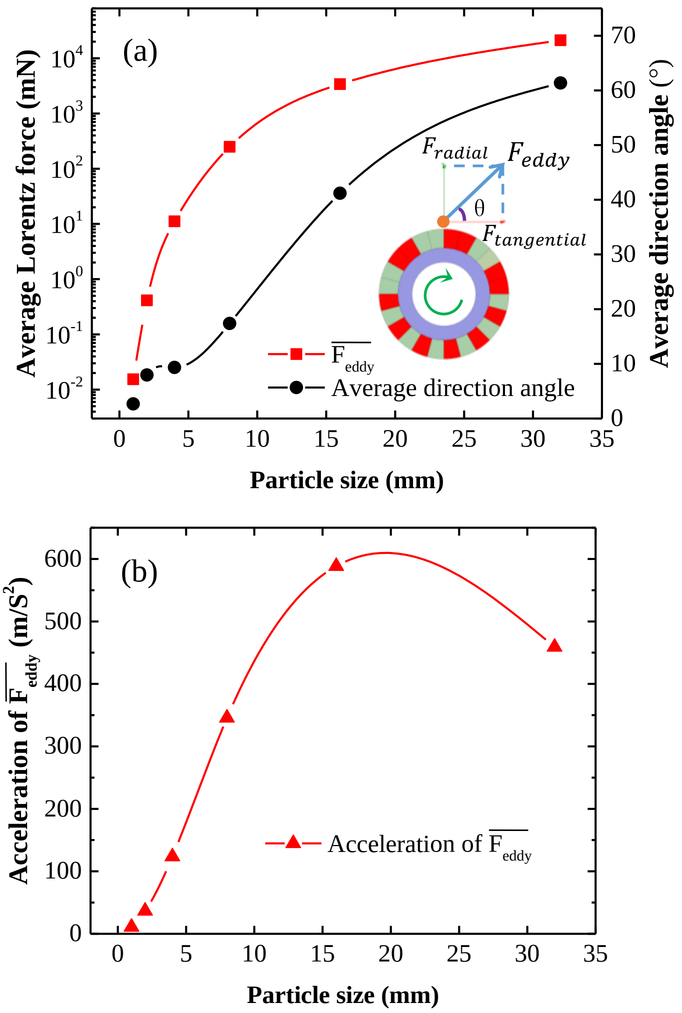

Fig. 2. The effect of particle size on the translational motion: the variation of average Lorentz force, average direction angle (a) and average acceleration (b) of Al particle with particle size when the rotational speed is 3600 rpm

Fig. 2 (a) shows the variation of the average Lorentz force ($\overline{F_{eddy}}$) and the average direction angle ($\bar{\theta}$) of Al particles with the particle size when the rotational speed is 3600 rpm. It shows that the increase of $\overline{F_{eddy}}$ spans several orders of magnitude with the increase of particle size. Therefore, a semi-logarithmic scale is used in the vertical axis on the left in the figure. This indicates that particle size is one of the most important factors affecting the Lorentz force. In fact, the dependence of the Lorentz force on the particle size is an important reason for the difficult separation of fine particles. The direction angle (θ) of the Lorentz force will also has a greater impact on the particle trajectory, but no study has concerned this issue so far. In a common belted-drum ECS, non-ferrous metal particles enter the separation area along the circumferential direction of the magnetic roller surface, and the particles do the projectile motion under the action of Lorentz force. When the Lorentz force is constant, the closer the direction angle is to 45˚, the greater the repulsion distance of the non-ferrous metal particles [31]. For the vertical rotary-drum ECS, the non-ferrous metal particles enter the separation area along the generatrix direction of the magnetic roller surface, and the particles do horizontal throwing motion when subjected to the Lorentz force. In this case, the direction angle also has a direct impact on the radial repulsion distance and the circumferential deflection of the non-ferrous metal particles. When the Lorentz force is constant, the closer the direction angle is to 90˚, the greater the repulsion distance of non-ferrous metal particles. Fig. 2 (a) shows that the direction angle of the Lorentz force also increases with the increase of the particle size, which also explains the low separation efficiency of small particles. This may be because the magnetic field gradient in the radial direction near the surface of the magnetic roller is larger than that in the tangential direction, and the magnetic field gradient is closely related to the magnitude of the Lorentz force [32]. In this case, when the particle size increases, the radial Lorentz force (F_{radial}) increases more than the tangential Lorentz force ($F_{tangential}$), and the direction angle of the Lorentz force increases accordingly.

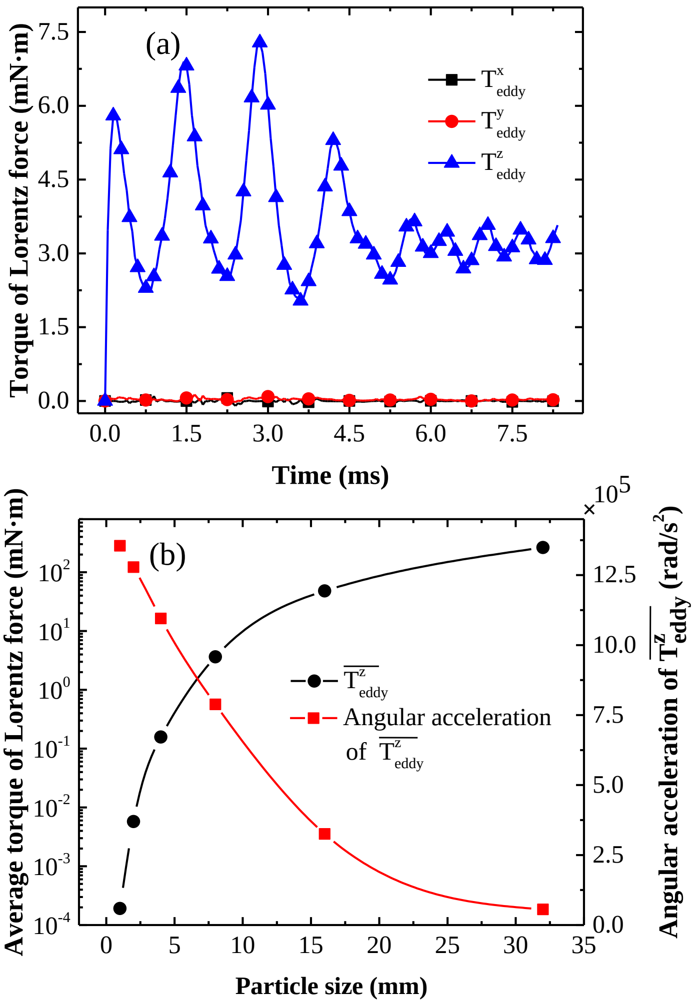

Fig. 3. The effect of particle size on the rotational motion: (a) the variation of the torque of Lorentz force of aluminium particle (8 mm) with time under the rotational speed of 3600 rpm; (b) the variation of the average torque of Lorentz force and its angular acceleration with the particle size at 3600 rpm.

The translational motion of non-ferrous metal particles with different particle sizes under Lorentz force is also related to their own mass. Thus the acceleration of particles by Lorentz force was investigated to eliminate the interference of the particle mass. Fig. 2 (b) shows the variation of the acceleration of $\overline{F_{eddy}}$ on the Al particle with the particle size under the rotational speed of 3600 rpm. It shows that when the particle size increases, the acceleration of non-ferrous metal particles does not increase continuously like the Lorentz force. Instead, a peak was observed when the particle size is about 19 mm in this case. This indicates that there may be an optimal separation particle size under specific structural parameters and operating parameters. These results are consistent with the changing trend of the repulsion distance based on an analytic model [33], which shows that the acceleration of Lorentz force can better reflect the actual separation effect than Lorentz force.

When dealing with the problem of difficult separation of fine particles, the torque of Lorentz force causing the rotational motion of non-ferrous metal particles has gradually attracted attention in the design of some new eddy current separator [8]. Fig. 3 (a) shows the variation of torque of Lorentz force components on an 8 mm diameter Al particle with time at 3600 rpm. The x, y, and z in the figure are the three axes of the local coordinate system with the origin at the particle center, and T_{eddy}^{x}, T_{eddy}^{y}, and T_{eddy}^{z} are the components of torque of Lorentz force in the triaxial direction respectively. It shows that the component of torque of Lorentz force about the x and y axes is almost zero, while the component of torque of Lorentz force about the z axis fluctuates with time. The large fluctuations correspond to the magnetic pole of NNSS, while the small fluctuations correspond to the magnetic pole of NS. This indicates that the fluctuates of T_{eddy}^{z} are due to the change of magnetic field distribution caused by the alternating structure of N and S poles in the circumferential direction of the magnetic roller. Meanwhile, there is no structural change in the axial direction of the magnetic roller, and the magnetic field is evenly distributed in the axial direction. The axial Lorentz force on the internal parts of the non-ferrous metal particle is almost zero, so the components of the torque of Lorentz force on the x and y axes are also close to zero, as expected. Similar phenomena can be found when investigating the variation of each component of torque of Lorentz force with time under other conditions. Thus T_{eddy}^{z} can be used as an accurate approximation for the total torque acting on the particle.

When studying the actual effect of the torque of Lorentz force on the rotational motion of the particles, it is necessary to eliminate the influence of the moment of inertia. Fig. 3 (b) shows the variation of average torque of Lorentz force ($\overline{T_{eddy}^{z}}$) and the corresponding angular acceleration (α) with particle size. The angular acceleration can be calculated according to $\overline{T_{eddy}^{z}} = I\alpha$, where I is the moment of inertia of the particle about an axis through the particle center. It shows that the average torque of Lorentz force increases with the increase of the particle size, and the angular acceleration corresponding to the average torque of Lorentz force decreases with the increase of the particle size. The results indicate that when the particle size decreases, the reduction rate of the moment of inertia is higher than that of the torque of Lorentz force, so the angular acceleration representing the intensity of the rotational motion has a continuous strengthening trend. Thus it can be seen that the torque of Lorentz force can be used to improve the separation efficiency of fine particles. These results can also be used to explain why the reversal of the magnetic roller can improve the separation efficiency of fine particles [34]. We should pay attention to the role of particle rotation when designing ECS for fine particles. Combining with the results of Fig. 2, it can be found that the Lorentz force and torque of non-ferrous metal particle increase significantly by 6 orders of magnitude with the increase of particle size. However, the increase of particle size will also cause the changes in mass and moment of inertia, so the acceleration and angular acceleration of particle can more directly reflect the translational and rotational motion of particles.

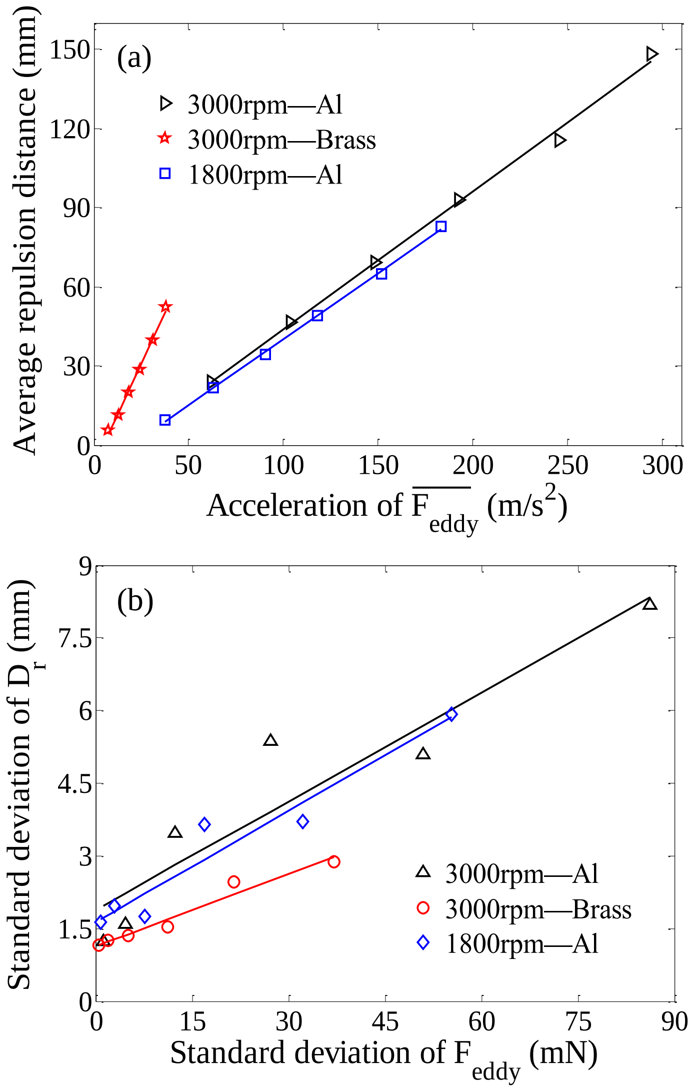

Fig. 4. Relationship between the simulation and the separation experiment under different particle sizes, material types and rotational speeds: (a) the relationship between the acceleration of $\overline{F_{eddy}}$ and the average repulsion distance; (b) the

relationship between the standard deviation of Lorentz force and the standard deviation of repulsion distance.

The relationships between the physical quantities in the simulation and the actual separation effect were investigated to justify the physical meaning of some quantities in the simulation and further verify the accuracy of the simulation model. The equipment used in the separation experiment is a vertical rotary-drum ECS, which achieves the separation based on the translational motion of non-ferrous metal particles caused by Lorentz force. Thus the relationship between the Lorentz force and the repulsion distance was investigated. The simulations and separation experiments included in Fig. 4 adopted the same experiment parameters (see Table 2 presented earlier in section 2.2), and Table 3 is the Pearson correlation analysis and linear regression analysis results corresponding to Fig. 4. Fig. 4 (a) is the relationship between the average repulsion distance ($\overline{D_r}$) in the separation experiments and the acceleration of $\overline{F_{eddy}}$ in the simulations. It shows that there is a linear correlation between the average repulsion distance and the acceleration of $\overline{F_{eddy}}$ on non-ferrous metal particles under the same material type and rotational speed, and the trend lines of the same material type almost overlap each other. The results indicate that the acceleration of $\overline{F_{eddy}}$ is closely related to the average repulsion distance, so the acceleration of $\overline{F_{eddy}}$ is the key factor affecting the repulsion distance. It can be used to evaluate the separation effect between non-ferrous metals and non-metals just like the repulsion distance: The greater the acceleration of $\overline{F_{eddy}}$, the better the separation effect between non-ferrous metals and non-metals. Fig. 4 (b) is the relationship between the standard deviation of the repulsion distance in the separation experiments and the standard deviation of the Lorentz force in the simulations. Similarly, there is a linear correlation between the standard deviation of the repulsion distance and the standard deviation of the Lorentz force, and the trend lines of the same material type almost overlap each other. The results show that the standard deviation of Lorentz force can characterize the concentration degree of particle falling points as the standard deviation of repulsion distance. Therefore, the standard deviation of Lorentz force can be used as a reference value in evaluating the separation effect between different non-ferrous metals.

Table 3. Correlation and linear regression analysis for the relationship between simulations and physical experiments.

Category	Material type	Rotational speed (rpm)	R^2	Correlation coefficient
Analysis on $\overline{D_r}$ and acceleration of $\overline{F_{eddy}}$, Fig. 3(a)	Al	1800	0.9988	0.9994
		3000	0.9973	0.9986
	Brass	3000	0.9947	0.9973
Analysis on the standard deviation for D_r and F_{eddy}, Fig. 3(b)	Al	1800	0.9341	0.9665
		3000	0.8864	0.9415
	Brass	3000	0.9583	0.9789

The coefficient of determination (R^2) measures the fraction of the total variation in the dependent variable that is explained by the independent variable. The values of R^2 in Table 3 are all greater than 0.85, which indicates that the acceleration and fluctuation of the Lorentz force can explain most of the variation in the mean and standard deviation of the repulsion distance. The order of R^2 in Fig. 4 (b) is: 3000 rpm-Al<1800 rpm-Al<3000 rpm-Brass, which is mainly determined by the magnitude of the standard deviation of each group of experiments. For example, the standard deviation of the Lorentz force and the repulsion distance of the Al particle at 3000 rpm is the largest, then the randomness of this set of data is the largest, so the variation caused by random factors is also the largest. In addition, Table 3 shows that the correlation coefficients between physical quantities in the separation experiments and simulations are all greater than 0.94, reaching a very high degree of correlation. The results in Fig. 4 and Table 3 prove the physical meaning of the acceleration and standard deviation of the Lorentz force in the simulation, and also verify the accuracy of the three-dimensional transient simulation model of ECS. On this basis, a more detailed study on particle size can be carried out by using the simulation model.

3.2 The interaction effects between particle size and other factors

The major choke point of the eddy current separation technology is the low separation efficiency of fine particles. Studying the interaction effects between the material parameters (material type), operating parameters (rotational speed), structural parameters (magnetic pole arrangement) and the particle size can guide the design, optimization and process of eddy current separator for fine particles.

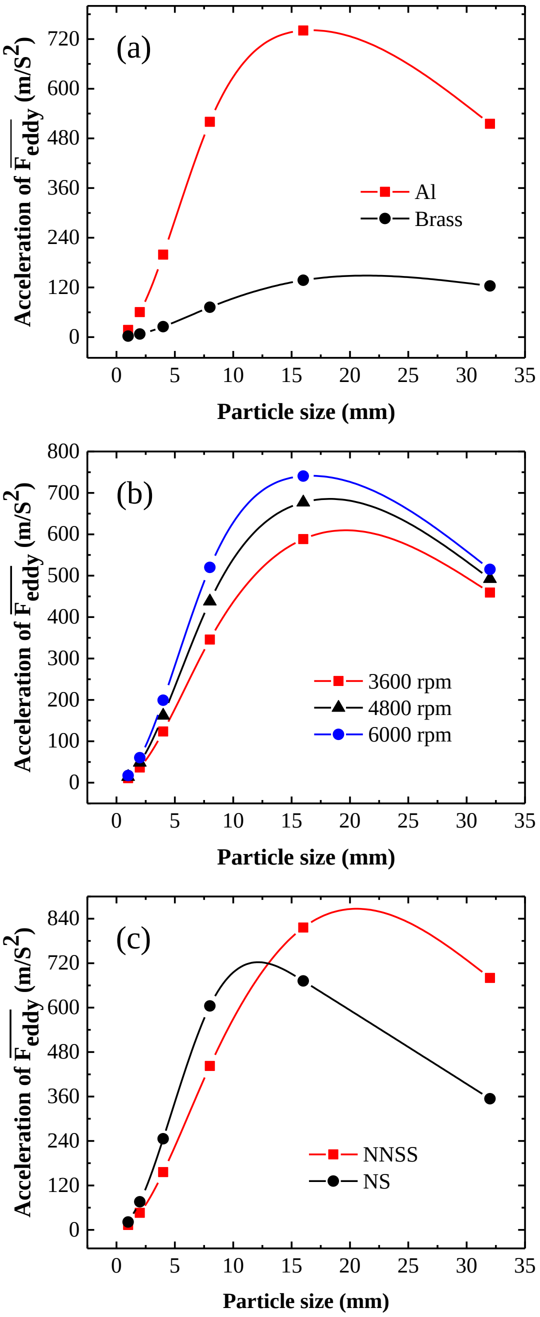

Fig. 5. The influence of the interaction effects on the acceleration of $\overline{F_{eddy}}$: (a) the variation of the acceleration of $\overline{F_{eddy}}$ on Al and brass particles with particle size when the rotational speed is 6000 rpm; (b) the acceleration of $\overline{F_{eddy}}$ on Al particle varies with particle size at different rotational speeds; (c) the variation of the

acceleration of $\overline{F_{eddy}}$ on Al particle with particle size under the two magnetic pole arrangements at a rotational speed of 6000 rpm.

Fig. 5 shows the influence of the interaction effects between the particle size and the material type, rotational speed, and magnetic pole arrangement on the acceleration of $\overline{F_{eddy}}$. It shows that the acceleration of $\overline{F_{eddy}}$ under various experimental conditions has a peak value, which corresponds to an optimal separation particle size. Thus the particle size range of the target mixture should be investigated before designing or optimizing the ECS, and then the parameters suitable for separating the mixture should be set according to the particle size range. Fig. 5 (a) shows the variation of the acceleration of $\overline{F_{eddy}}$ on Al and brass particles with particle size under the rotational speed of 6000 rpm. The ratio of electrical conductivity to density (σ/ρ) is an important indicator for evaluating material differences in eddy current separation, and the σ/ρ of Al and brass are 12.96 and 2.44, respectively [1]. It can be seen that the interaction effect between particle size and material type is significant. When the σ/ρ of the material is large, the particle size has a greater impact on the acceleration of $\overline{F_{eddy}}$. When the acceleration of $\overline{F_{eddy}}$ is constant, the material with higher σ/ρ corresponds to a smaller particle size. This indicates that the minimum sortable particle size decreases with the increase of σ/ρ. Hence, improving the conductivity of the material through low-temperature pretreatment or cooling after crushing [30] can reduce the minimum sortable particle size of ECS. Fig. 5 (b) is the variation of the acceleration of $\overline{F_{eddy}}$ on Al particle with particle size under different rotational speeds. It shows that there is also an interaction effect between the particle size and the rotational speed of magnetic roller. When the particle size is close to the optimal separation particle size, the influence of the rotational speed on the acceleration of $\overline{F_{eddy}}$ is more significant, and the particle sizes corresponding to a constant acceleration decrease with the increase of rotational speed. This indicates that increasing the rotational speed of magnetic roller or the frequency of alternating magnetic field can improve the separation efficiency of fine particles, which is consistent with the application experience of ECS in industry [35]. Fig. 5(c) shows the variation of the acceleration of $\overline{F_{eddy}}$ on Al particle with particle size under the two magnetic pole arrangements of NNSS and NS when the rotational speed is 6000 rpm. It shows that the peak value of NNSS is on the right of the peak value of NS. This indicates that NS is more suitable for separating fine particles, while NNSS has a better separation effect for large particles. In the practical application of eddy current separation technology, the non-uniform magnetic system combined with NNSS and NS is a very common magnetic roller structure (see Fig. 1(b)). It turns out that the non-uniform magnetic system can process mixtures with greater particle size differences and greatly increase the separable particle size range of ECS. In addition, the pole pitch of NNSS is twice that of NS, which is the essential difference between the two magnetic pole arrangements. When dealing with fine particles, a magnetic roller structure with a smaller pole pitch and a larger number of magnetic poles should be selected.

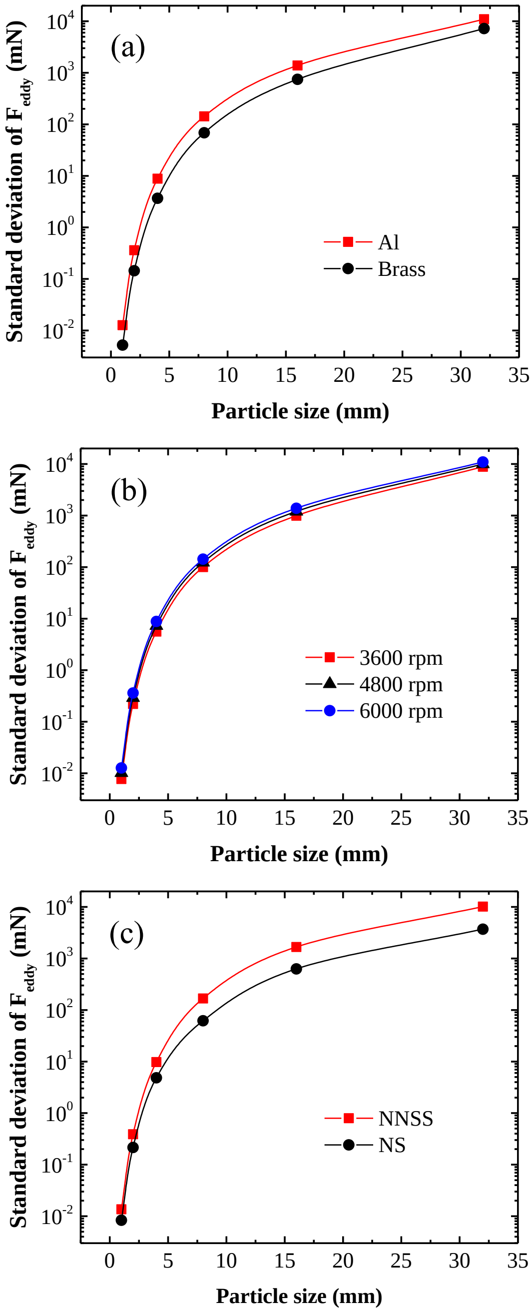

Fig. 6. The influence of the interaction effects on the standard deviation of Lorentz force: (a) the variation of the standard deviation of the Lorentz force on Al and brass particles with particle size when the rotational speed is 6000 rpm; (b) the standard deviation of the Lorentz force on Al particle varies with particle size at different rotational speeds; (c) the variation of the standard deviation of the Lorentz force on Al

particle with particle size under the two magnetic pole arrangements at a rotational speed of 6000 rpm.

Fig. 6 shows the influence of the interaction effects between the particle size and the material type, rotational speed and magnetic pole arrangement on the standard deviation of Lorentz force. It shows that the standard deviation of Lorentz force increases with the increase of particle size under various experimental conditions, indicating that large particle size will increase the randomness and distribution range of the falling points of non-ferrous metal particles. Fig. 5 (a) shows that the acceleration difference of Lorentz force between different non-ferrous metals (such as Al and brass) increases first and then decreases. Thus it can be deduced that with the increase of particle size, the average gap between the falling points of different non-ferrous metal particles first increases and then decreases. Meanwhile, the dispersion degree for the falling points of non-ferrous metal particles continues to increase, so the separation efficiency between different non-ferrous metals may increase slowly and then decrease sharply. Fig. 6 also shows that the dispersion degree of the falling points of non-ferrous metal particles increases with the increase in σ/ρ, rotational speed and pole pitch, which may have a negative impact on the separation between different non-ferrous metals. Among them, the influence of rotational speed is the weakest, and the influence of the magnetic roller structure is the most significant. The magnetic roller structure with a smaller pole pitch should be considered when separating the mixtures of different non-ferrous metals.

3.3 The mechanism of particle size affecting separation

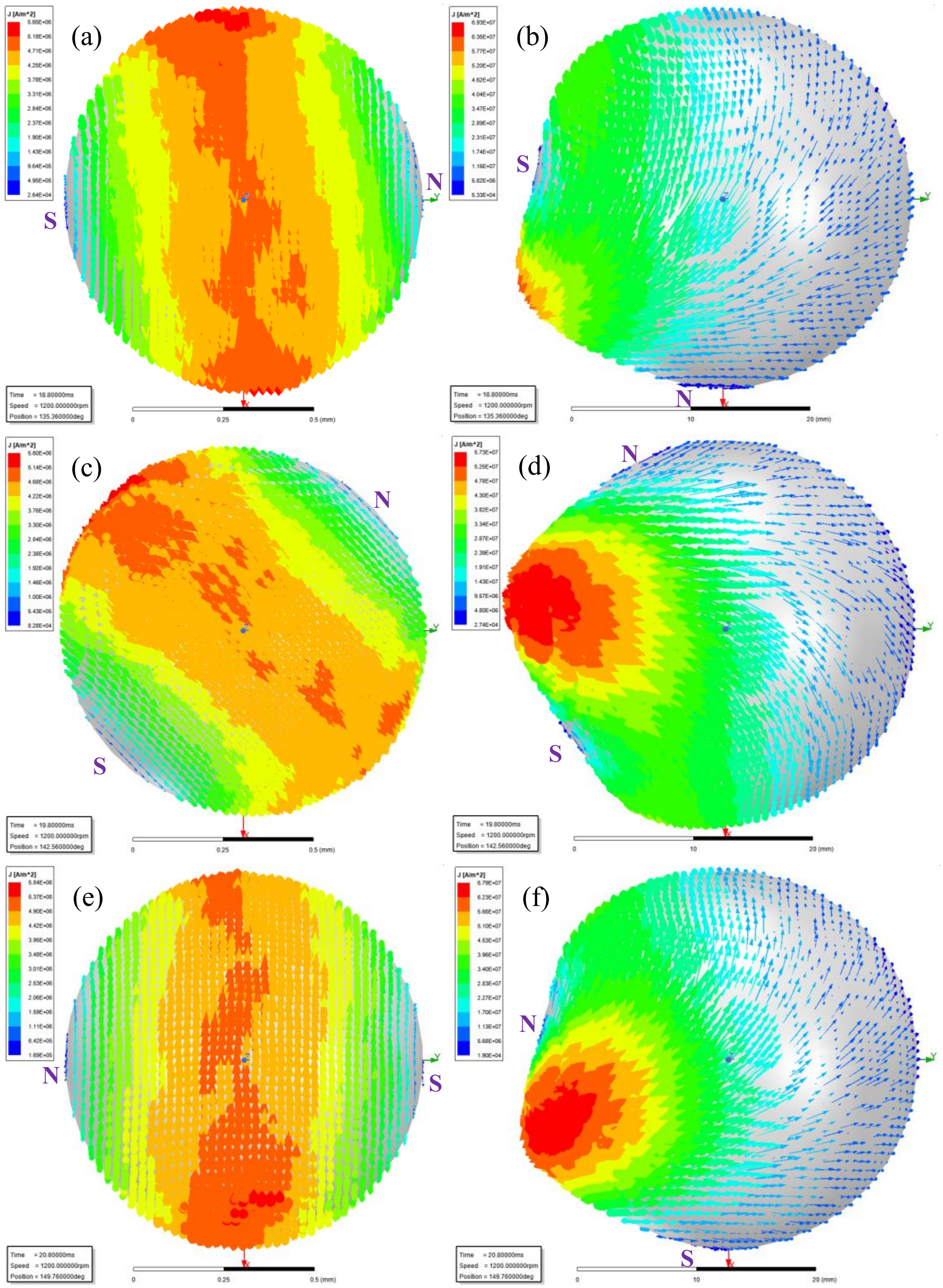

Fig. 7. The eddy current distribution of Al particles at 1200 rpm: (a) D=1 mm, t=18.8 ms; (b) D=32 mm, t=18.8 ms; (c) D=1 mm, t=19.8 ms; (d) D=32 mm, t=19.8 ms; (e) D=1 mm, t=20.8 ms; (f) D=32 mm, t=20.8 ms.

To further clarify the internal mechanism of particle size affecting separation, it is not enough to study the force on non-ferrous metal particles, and the electromagnetic process inside particles can also provide important information. In this regard, related research is mainly carried out through theoretical analysis. For example, a magnetic dipole model [32] was proposed based on theoretical derivation, in which the Lorentz force ($F_{eddy} = m \cdot \nabla\mathrm{B}$) on the non-ferrous metal particle mainly depends on the magnetic moment (m) of the non-ferrous metal particle and the magnetic field gradient ($\nabla\mathrm{B}$). The magnetic moment is closely related to the eddy current distribution in the non-ferrous metal particles. Therefore, the influence of particle size on eddy current distribution and magnetic field gradient is investigated in this section.

Fig. 7 shows the eddy current distributions of Al particles with particle size of 1 mm and 32 mm at three different instants (18.8 ms, 19.8 ms and 20.8 ms) under a rotational speed of 1200 rpm. The three instants happen when the Al particle are facing the NS junction, the middle of S pole and the SN junction on the magnetic roller, respectively. It can be seen from Fig. 7 that the eddy current of 1 mm Al particles is more evenly distributed on the particle. The main flow of eddy current circulates around the maximum cross-section of the particles, and the N pole and S pole are located at two symmetrical ends on the particle, thus forming an analogue of a magnetic dipole. The magnetic moment is determined by the following equation [33, 36].

$$\mathbf{m} = \frac{1}{2}\int_V \mathbf{r} \times \mathbf{j}\, dV \tag{4}$$

where $\mathbf{m}$ is the magnetic moment of the particle, $\mathbf{r}$ is the coordinate vector with respect to the centre of the mass particle, and $\mathbf{j}$ is the eddy current density in the particle. According to the formula of the magnetic moment for a magnetic dipole, the magnetic moment is proportional to the eddy current intensity and the area surrounded by the eddy current loop. Fig. 7 shows that the diameter and the eddy current intensity of the 32 mm Al particle are one order of magnitude larger than that of the 1 mm Al particle, so the Lorentz force generated in a larger non-ferrous metal particle is also larger. In the range of small particle size, the eddy current intensity of the particle increases with the increase of particle size, and the eddy current distribution is uniform because the whole particle is contained in the effective area of magnetic field. In this case, the growth rate of Lorentz force is higher than that of particle mass with the increase of particle size, and the acceleration of Lorentz force increases with the particle size. When the particle size increases to a certain extent, the magnetic field intensity on each part of the particle is uneven due to the rapid attenuation of the magnetic field near the surface of the magnetic roller. The part far away from the magnetic roller on the particle exceeds the effective area of magnetic field, so the eddy current is unequally distributed on the particle. Specifically, the main flow of eddy current doesn't circulate around the maximum cross-section of the particle like the case of the small size, but concentrates on the side close to the magnetic roller. The N pole and S pole are also lean to this side, which leads to a smaller area surrounded by the eddy current loop. And the magnetic moment of the electric current loop with a smaller surrounding area is smaller. Thus, the growth rate of Lorentz force will be less than that of particle mass if the particle size further increases. In this case, the acceleration of Lorentz force gradually decreases, which has a negative impact on the separation of large particles. In addition, the uneven distribution of the eddy current in non-ferrous metal particles will further aggravate the instability of the Lorentz force, so the standard deviation of the Lorentz force increases greatly, which brings difficulties to the separation between different non-ferrous metals. NNSS is significantly larger than NS in terms of the effective area of the magnetic field. This study also compared the eddy current distribution of the Al particles under the two magnetic pole arrangements of NNSS and NS to further verify the above reasons for the uneven distribution of eddy current. The result is similar to the comparison of the eddy current distribution of particles with different sizes. The uneven distribution of eddy current on the Al particles under NS magnetic system is more significant. In the design and optimization process of ECS, the particle size range of the target material should be investigated first, and then ensure that the entire non-ferrous metal particle is included in the effective area of the magnetic field. In this way, the problem of uneven distribution of eddy current can be avoided.

To accurately evaluate the magnitude of the magnetic field gradient in the space where the non-ferrous metal particle is located, the volume integral of the magnetic field gradient inside the particle is used to quantify the magnetic field gradient intensity. The magnetic field gradient integral ($\nabla\mathbf{B}_{VI}$) can be expressed by the following formula.

$$\nabla\mathbf{B}_{VI} = \iiint \nabla\mathbf{B}(\mathrm{x}, \mathrm{y}, \mathrm{z})\mathrm{dV} \tag{5}$$

where $\nabla\mathbf{B}(\mathrm{x}, \mathrm{y}, \mathrm{z})$ is the magnetic field gradient at position $(\mathrm{x}, \mathrm{y}, \mathrm{z})$. Fig. 8 is the variation of the time-average of the magnetic field gradient integration in the non-ferrous metal particle with particle size. It shows that the magnetic field gradient in the region occupied by the particle increases with the increase of particle size. The results in Fig. 7 and Fig. 8 show that with the decrease of particle size, the magnetic gradient in the particle and the magnetic moment formed by eddy current will decrease significantly, resulting in the rapid reduction of the Lorentz force on the non-ferrous metal particle, and the power relationship between the Lorentz force and particle size is higher than the cubic relationship between mass and particle size ($m = \rho \cdot \frac{4}{3}\pi r^3$). Although fine particles can be completely contained in the effective area of the magnetic field, and the main flow of eddy current in fine particles can circulate the maximum cross-section of particles. Still, the reduction speed of the Lorentz force is higher than that of particle mass when the particle size decreases. Therefore, the acceleration of Lorentz force gradually decreases, and gravity, aerodynamic drag force [37], etc. gradually occupy a dominant position in determining the particle trajectory, which causes the problem of difficult separation of fine particles. Based on the above analysis of large and fine particles, it can better explain why there is an optimal particle size for a specific eddy current separator. The results also indicate that the magnetic field gradient in the spatial region of the target mixture should be enhanced as much as possible in the design and optimization of the magnetic roller.

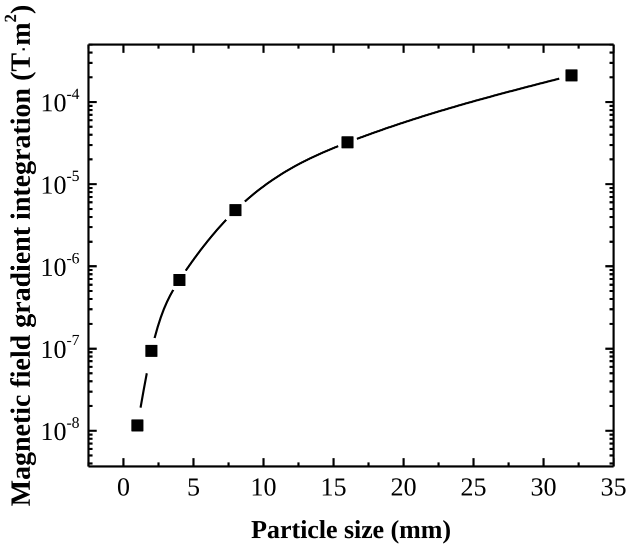

Fig. 8. The variation of the time-average of the magnetic field gradient integration in the non-ferrous metal particle with particle size.

4. Conclusion

The influence rule of the particle size on the eddy current separation, and the mechanisms involved, are of critical importance for the efficient utilization of ECS technology in various mixtures. These issues were studied by combining the numerical simulations and the separation experiments. The correlation coefficients between the physical quantities in the simulations and the performance indexes from the separation experiments are all greater than 0.94. This further validates the three-dimensional transient simulation model of ECS used. The main conclusions can be summarized as follow:

(1) With the decrease of particle size, the translational motion of non-ferrous metal particles increases first and then decreases rapidly, while the rotational motion continues to increase. To improve the separation efficiency of fine particles, the rotational speed and the σ/ρ should be increased, the pole pitch should be reduced,

and the rotational motion of the particles should be utilized efficiently.

(2) The particle size determines separation efficiency by affecting the magnitude and distribution uniformity of eddy currents. When designing and optimizing the ECS, the particle size range of the target mixture should be investigated in advance, and the particles should be within the effective area of the magnetic field. Meanwhile, the magnetic field gradient of the space region occupied by the particles should be increased as much as possible.

These results can provide guidance for the design and optimization of ECS for fine particles such as the electronic waste and the incineration bottom ash, which may also expand the new application areas for this green technology.

Acknowledgments

The authors are grateful to the financial support provided by the National Key R&D Program of China (Grant No. 2021YFA1600204) and the Fundamental Research Funds for the Central Universities (Grant Nos. N2109002 and N2025035). Cao Bin holds a scholarship provided by the China Scholarship Council during the study at Bournemouth University.

References

[1] J. Cui, E. Forssberg, Mechanical recycling of waste electric and electronic equipment: a review, J. Hazard. Mater., 99 (2003) 243-263.

[2] S.K. Padamata, A. Yasinskiy, P. Polyakov, A Review of Secondary Aluminum Production and Its Byproducts, JOM, 73 (2021) 2603-2614.

[3] B. Yan, R. Liang, B. Li, J. Tao, G. Chen, Z. Cheng, Z. Zhu, X. Li, Fast identification and characterization of residual wastes via laser-induced breakdown spectroscopy and machine learning, Resour. Conserv. Recycl., 174 (2021).

[4] M. Constant, N. Coppin, F. Dubois, R. Artoni, J. Lambrechts, V. Legat, Numerical investigation of the density sorting of grains using water jigging, Powder Technol., 393 (2021) 705-721.

[5] H. Louati, N. Zouzou, A. Tilmatine, A. Zouaghi, R. Ouiddir, Experimental investigation of an

electrostatic adhesion device used for metal/polymer granular mixture sorting, Powder Technol., 391 (2021) 301-310.
[6] J. Xia, Z. Lei, K. Jiang, Q. Wang, J. Ku, Q. Yan, Comparison of various forces acting on magnetic particles in a low-intensity magnetic field: A 3D FEA, Powder Technol., 401 (2022).
[7] Y. Li, X. Qin, Z. Zhang, H. Dong, Operation parameters optimization of a separating system for non-ferrous metal scraps from end-of-life vehicles based on coupled simulation, Waste Manage., 120 (2021) 667-674.
[8] Y.R. Smith, J.R. Nagel, R.K. Rajamani, Eddy current separation for recovery of non-ferrous metallic particles: a comprehensive review, Miner. Eng., 133 (2019) 149-159.
[9] J. Ruan, Y. Qian, Z. Xu, Environment-friendly technology for recovering nonferrous metals from e-waste: eddy current separation, Resour. Conserv. Recycl., 87 (2014) 109-116.
[10] E.R. Rene, M. Sethurajan, V. Kumar Ponnusamy, G. Kumar, T.N. Bao Dung, K. Brindhadevi, A. Pugazhendhi, Electronic waste generation, recycling and resource recovery: Technological perspectives and trends, J. Hazard. Mater., (2021).
[11] F. Huber, Modelling of material recovery from waste incineration bottom ash, Waste Manag, 105 (2020) 61-72.
[12] X.M. Di WANG, Xiongfei ZHI, Shuming ZHANG, Research Review of Scrap Metals Eddy Current Separation Technology, Sensors & Transducers, (2013).
[13] L.N. Pham, G.F. Tabor, A. Pourkand, J.L.B. Aman, T. Hermans, J.J. Abbott, Dexterous magnetic manipulation of conductive non-magnetic objects, Nature, 598 (2021) 439-443.
[14] Z.H. Xia Yi, Shao Liming, He Pinjing, Speciation and recoverability of valuable metals in municipal solid waste incineration bottom ash, Research of Environmental Sciences, 30 (2017) 586-591.
[15] M. Kaya, Recovery of metals and nonmetals from electronic waste by physical and chemical recycling processes, Waste Manage., 57 (2016) 64-90.
[16] H. Naidu, Electrodynamic separation of metallic granules from mixed waste stream, Environmental Engineering, University of Utah, 2010.
[17] N. Dholu, J.R. Nagel, D. Cohrs, R.K. Rajamani, Eddy current separation of nonferrous metals using a variable-frequency electromagnet, KONA Powder Part. J., 34 (2017) 241-247.
[18] Y. Weichao, Z. Zhu, Z. Chang, L. Zhao, z. dai, K. Zhang, F. Ning, G. Zhang, Z. Hou, M. Wang, x. zhang, z. wang, Development of an eddy-current separation equipment with high gradient superconducting magnet, IEEE Trans. Appl. Supercond., 25 (2014) 1-4.
[19] F. Settimo, P. Bevilacqua, P. Rem, Eddy Current Separation of Fine Non-Ferrous Particles from Bulk Streams, Physical Separation in Science and Engineering, 13 (2004) 15-23.
[20] M.-x. Hao, Y.-h. Zhang, Y. Huang, H.-l. Wang, H. Li, J.-q. Du, W.-j. Lv, J.-p. Li, P.-b. Fu, J.-w. Wu, Effect of particle self-rotation on separation efficiency in mini-hydrocyclones, Powder Technol., 399 (2022).
[21] M. Lungu, A. Neculae, Eddy current separation of small nonferrous particles using a complementary air-water method, Sep. Sci. Technol., 53 (2017) 126-135.
[22] R. Meier-Staude, Z. Schlett, M. Lungu, D. Baltateanu, A new possibility in Eddy-Current separation, Miner. Eng., 15 (2002) 287-291.
[23] M. Lungu, P. Rem, Eddy-current separation of small nonferrous particles by a single-disk separator with permanent magnets, IEEE Trans. Magn., 39 (2003) 2062-2067.
[24] F. Ye, X. Ren, G. Liao, T. Xiong, J. Xu, Mathematical model and experimental investigation for

eddy current separation of nonferrous metals, Results Phys., 17 (2020) 103170.

[25] S. Roy, V. Ari, J. Konar, A. Das, Metal enrichment of finely ground electronic waste using eddy current separation, Sep. Sci. Technol., 47 (2012) 1777-1784.

[26] B. Cao, Y. Yuan, Y. Arman, L. Feng, Z. Zhou, T. Wang, Q. Wang, Optimization of Halbach magnetic roller for eddy current separation based on the response surface method and multi-objective genetic algorithm, J. Clean. Prod., 278 (2021).

[27] Z. Huang, J. Zhu, X. Wu, R. Qiu, Z. Xu, J. Ruan, Eddy current separation can be used in separation of non-ferrous particles from crushed waste printed circuit boards, J. Clean. Prod., 312 (2021).

[28] S. Zhang, P.C. Rem, E. Forssberg, Particle trajectory simulation of two-drum eddy current separators, Resour. Conserv. Recycl., 26 (1999) 71-90.

[29] A.N.E.I. Ayad, M. Larab, H. boudjella, F. Benhamida, Simulation of eddy current and repulsive force of non-ferrous particles in eddy current separator, Prz. Elektrotechniczny, 1 (2019) 49-52.

[30] Y. Yi, C. Bin, Z. Xuemei, F. Lei, W. Tiansheng, W. Qiang, Effects of material temperature on the separation efficiency in a rotary-drum type eddy current separator, Powder Technol., 404 (2022).

[31] D.M. Katz, Physics for scientists and engineers: foundations and connections with modern physics, Cengage Learning, Boston, 2015.

[32] P.C. Rem, P.A. Leest, A.J.V. Den Akker, A model for eddy current separation, Int. J. Miner. Process., 49 (1997) 193-200.

[33] J.R. Nagel, An analytic model for eddy current separation, Miner. Eng., 127 (2018) 277-285.

[34] S. Zhang, P.C. Rem, E. Forssberg, The investigation of separability of particles smaller than 5 mm by eddy current separation technology. part I: rotating type eddy current separators, Magn. Electr. Sep., 9 (1999) 233-251.

[35] M. Syc, F.G. Simon, J. Hyks, R. Braga, L. Biganzoli, G. Costa, V. Funari, M. Grosso, Metal recovery from incineration bottom ash: state-of-the-art and recent developments, J. Hazard. Mater., 393 (2020) 122433.

[36] M. Lungu, Separation of small nonferrous particles using a two successive steps eddy-current separator with permanent magnets, Int. J. Miner. Process., 93 (2009) 172-178.

[37] R. Bunge, Recovery of metals from waste incinerator bottom ash, 2015.